SureSeq

Development and Analytical Evaluation of a Targeted RNA-Based Fusion Assay for Measurable Residual Disease (MRD) Assessment

Lucy Georgieva, Tom Huckvale, James Reid, Jolyon Holdstock, Matthew Rooney, Jackie Chan, Graham Speight Oxford Gene Technology (OGT).

A Sysmex Group Company

What binds us, makes us.

Introduction

Fusion genes are key drivers of many cancers, particularly myeloid malignancies. While fusion detection has traditionally relied on fluorescence *in situ* hybridisation (FISH) and reverse transcription polymerase chain reaction (RT-qPCR), use of targeted next-generation sequencing (NGS) is increasingly used to characterise a broad range of relevant targets in a single assay without prior knowledge of the fusion type. Measurable Residual Disease (MRD) assessment requires longitudinal, sensitive quantification of ultra-low abundance fusion transcripts. In this study we assessed the capability of OGT's SureSeq™ myPanel Myeloid Fusion MRD Panel to detect a range of fusion types at levels suitable for MRD assessment.

Methods

Workflow

Contrived RNA was converted to cDNA, followed by library generation and target enrichment (Figure 1). Enriched libraries were sequenced on an Illumina NextSeq, 2 x 150bp.

Panel

The SureSeq myPanel Myeloid Fusion MRD Panel targets approximately 30 myeloid fusions relevant to AML research. Hybrid capture baits support agnostic partner detection (Table 1).

Samples

This study utilised 16 commercially available fusion-positive cell lines with a range of known fusions targeted by the panel including *KMT2A* rearrangements, *BCR::ABL1*, *PML::RARA*, *RUNX1::RUNX1T1*, *ETV6::RUNX1* as well as rare fusions. A further 4 control samples were used as negative controls. Serial dilutions in a fusion-negative control down to 4.0 log_{10} reduction from the neat samples (equivalent to a 1 in 10,000 dilution) to establish MRD level detection levels.

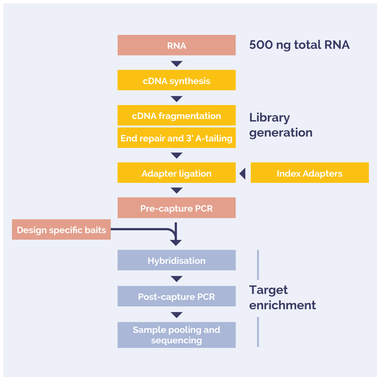


Figure 1. RNA sample to sequencing in 2 days with minimal hands-on time.

SureSeq Myeloid MRD Fusion Panel				
RBM15::*MKL1* (*RBM15::MRTFA*) t(1;22)(p13.3;q13.3)	***PICALM***::*MLLT10* t(10;11)(p12.3;q14.2)	***KMT2A***::*NEBL* t(10;11)(p12.3;q23.3)	***RUNX1***::*RUNX1T1* (*AML1::ETO*) t(8;21)(q21..3;q22.1)	***FGFR1***::*ZMYM2* t(8;13)(p11;q12)
(*GATA2*::***EVI1*** (*GATA2::**MECOM***)) inv(3)(q21.3q26.2) *"via MECOM overexpression"*	***KMT2A***::*MLLT3* (*AF9*) t(9;11)(p21.3;q23.3)	***PML***::***RARα*** (*PML::RARA*) t(15;17)(q24;q21)	***ETV6***::***RUNX1*** (*TEL::AML1*) t(12;21)(p13.2;q22.1)	*FIP1L1*::***PDGFRA*** del(4)(q12q12)
RPN1::***EVI1*** (*RPN1::MECOM*) inv(3)(q21q26) *"via MECOM overexpression"*	***KMT2A***::*ELL* t(11;19)(q23.3;p13.11)	*KAT6A*::***CREBBP*** t(8;16)(p11.2;p13.3)	***RUNX1***::***MECOM*** (*AML1::EVI1*) t(3;21)(q26.2;q22.1)	***PDGFRB***::*EBF1* del(5)(q32q33)
DEK::***NUP214*** (*DEK::CAN*) t(6;9)(p22.3;q34)	***KMT2A***::*MLLT1* (*ENL*) t(11;19)(q23.3;p13.3)	*PCM1*::***JAK2*** t(8;9)(p22;p24)	***BCR***::***ABL1*** t(9;22)(q34.1;q11.2)	***PDGFRB***::*TNIP1* t(5;5)(q32;q33)
NUP98::*NSD1* t(5;11)(q35;p15.4)	***KMT2A***::*MLLT4* (*KMT2A::AFDN*) t(6;11)(q27;q23.3)	***FUS***::*ERG* t(16;21)(p11.2;q22.2)	*NPM1*::***MLF1*** t(3;5)(q25.32;35.1)	***PDGFRB***::*ATF7IP* t(5;12)(q32;p13.1)
NUP98::*HOXA9* t(7;11)(p15.2;p15.4)	***KMT2A***::*MLLT11* t(1;11)(q21.3;q23.3)	***CBFB***::*MYH11* inv(16)(p13.1q22)	***FGFR1***::***BCR*** t(8;22)(p11;q11.2)	***PDGFRB***::***ETV6*** t(5;12)(q32;p13.2)

Table 1: 30 of the most relevant fusions for AML research are targeted by the SureSeq myPanel Myeloid Fusion MRD Panel.

Data analysis

Sequencing data was analysed using OGT's cloud-based Interpret software. Unique molecular identifiers (UMI) based deduplication enabled sensitive fusion detection, with exon-level breakpoint resolution. Fusion detection is confirmed by the presence of ≥5 UMI-deduplicated supporting reads that span the fusion breakpoint. Detection of translocations in *MECOM* are reported as overexpression in the software.

Results I

Fusions detected at MRD-levels

All expected fusions targeted by the panel were detected as shown by the presence of deduplicated supporting reads covering the fusion breakpoints, see Tables 2 and 3.

Highly expressed fusions including *RUNX1::RUNX1T1* (KASUMI-1), *ETV::RUNX1* (REH), & *ETV6::ABL2* (HT93), remained detectable at a 4.0 log_{10} reduction (1 in 10,000 dilution), with ≥ 5 supporting reads reported by the pipeline. *BCR::ABL1* (K562) and *FUS::ERG* (YNH-1) fusions were detected at 3.7 log_{10} reduction (1 in 7,500 dilution). The results demonstrate the suitability of this NGS assay for MRD assessment (Table 2).

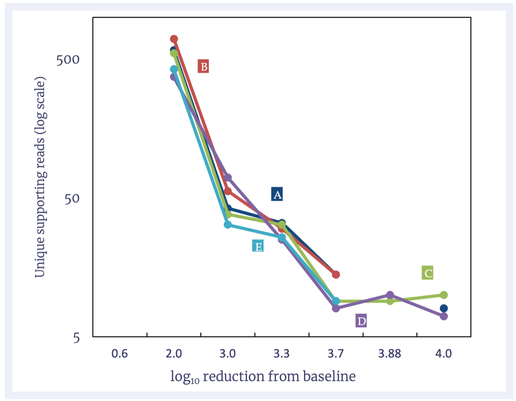


Figure 2: Plot showing highly expressed fusions remaining detectable for KASUMI-1, REH and HT93 cell-lines when RNA is diluted to 4.0 log_{10} reduction from baseline. K562 and YNH-1 expected fusions were detectable at a 3.7 log_{10} reduction from baseline.

	Cell-line	Expected fusion	Translocation	Breakpoint location determined by NGS	Log_{10} reduction
A	HT93	*ETV6::ABL2*	t(1;12)(q25;p13.2)	chr12:11869969 chr1:179133374	4.0
B	K562	*BCR::ABL1*	t(9;22)(q34.1;q11.2)	chr22:23290412 chr9:130854064	3.7
C	KASUMI-1	*RUNX1::RUNX1T1*	t(8;21)(q21..3;q22.1)	chr21:34859474 chr8:92017363	4.0
D	REH	*ETV6::RUNX1*	t(12;21)(p13.2;q22.1)	chr12:11869969 chr21:34892963	4.0
E	YNH-1	*FUS::ERG*	t(16;21)(p11.2;q22.2)	chr16:31186836 chr21:38383923	3.7

Table 2. 5 cell-lines exhibited highly expressed fusions, which remained detectable at 3.7 – 4.0 log_{10} reduction from baseline.

Results II

Range of fusion types

In the remaining cell lines, fusion-supporting reads were detected between 2.0 -3.3 log_{10} reduction (1 in 100 to 1 in 2,000 dilution) demonstrating a broad range of fusion types reported, with NGS able to identify the breakpoint location of each.

Cell-line	Expected fusion	Translocation	Breakpoint location determined by NGS	Log_{10} reduction
AP-1060	*ETV6::NTRK3*	t(12;15)(p13.2;q25.3)	chr12:11853561 chr15:87981360	2.0
AP-1060	*PML::RARa*	t(15;17)(q24;q21)	chr15:74033414 chr17:40348316	3.3
EOL-1	*FIP1L1::PDGFRA*	del(4)(q12q12)	chr4:54274925 chr4:53425965	0.6
HNT-34	*BCR::ABL1*	t(9;22)(q34.1;q11.2)	chr22:23290412 chr9:130854064	3.3
HT93	*PML::RARa*	t(15;17)(q24;q21)	chr15:74033408 chr17:40348316	3.3
KG-1	*FGFR10P2::FGFR1*	t(8;12)(p11;p11.23)	chr8:38418373 chr12:26957743	2.0
ME-1	*CBFB::MYH11*	inv(6)(p13.1q22)	chr16:67082308 chr16:15721051	2.0
ML-2	*KMT2A::AFDN*	t(6;11)(q27;q23.3)	chr11:118482495 chr6:167864551	3.3
NOMO-1	*KMT2A::MLLT3*	t(9;11)(p21.3;q23.3)	chr11:118484314 chr9:20365744	3.0
REH	*RUNX1::PRDM7*	t(16;21)(q24.3;q22.1)	chr21:35048842 chr16:90062502	3.0
SHI-1	*KMT2A::AFDN*	t(6;11)(q27;q23.3)	chr11:118482495 chr6:167864551	3.0
SKNO-1	*RUNX1::RUNX1T1*	t(8;21)(q21..3;q22.1)	chr21:34859474 chr8:92017363	3.3
THP-1	*KMT2A::MLLT3*	t(9;11)(p21.3;q23.3)	chr11:118482495 chr9:20365744	3.0
U-937	*PICALM::MLLT10*	t(10;11)(p12.3;q14.2)	chr11:85983973 chr10:21617207	0.6

Table 3: All expected fusions were detected with the assay, at a range of expression levels.

Results III

MECOM expression

MECOM expression was detected down to 4.0 log_{10} reduction in the cell-line HNT-34 (Figure 3). Detection of this expression level is important for identifying *MECOM* translocations, for example inv(3)(q21q26) and t(3;3)(q21;q26). Normalised expression levels of *MECOM* were reported in Interpret alongside the reported fusions.

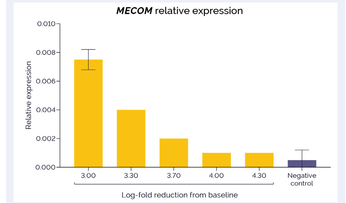


Figure 3. Relative expression of *MECOM* across serial log-fold reductions from baseline in HNT-34.

Results IV

Partner agnostic detection

The SureSeq myPanel Myeloid Fusion MRD Panel uses RNA-based, partner-agnostic detection to identify KMT2A rearrangements in a single workflow. Across multiple cell-line models, fusion-supporting reads were detected for *KMT2A::AFDN* and *KMT2A::MLLT3*, with reads and breakpoint localisation retained after a 3.0 log_{10} reduction in RNA input versus the neat sample. This supports sensitive detection of common, rare and potentially novel *KMT2A* fusions across diverse partners.

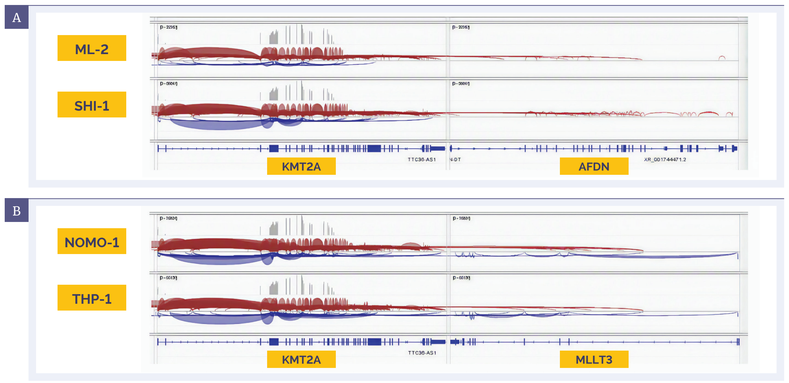


Figure 4. Split view in IGV showing fusion reads across two genes A Panel A :shows unique supporting reads for *KMT2A::AFDN* fusions in ML-2 and SHI-1 cell lines when diluted 3.0 log_{10} reduction from baseline; B panel B shows unique supporting reads for the *KMT2A::MLLT3* fusion in NOMO-1 and THP-1 cell lines.

Conclusions

- These results demonstrate the suitability of OGT's SureSeq myPanel Myeloid Fusion MRD Panel for the sensitive MRD assessment of fusion transcripts relevant to AML research.
- All expected fusion transcripts were detected across the cohort, with breakpoint locations accurately identified by Interpret software at exon-level resolution.
- The assay supports monitoring of *MECOM* translocation events through sensitive detection of *MECOM* overexpression, with measurable expression maintained following a 4.0 log_{10} reduction in HNT-34 cell-line RNA.
- Partner-agnostic analysis enabled identification of distinct *KMT2A* fusion partners within a single workflow, while both fusion transcripts and *MECOM* expression remained measurable across serial dilutions.
- These findings highlight the suitability of targeted RNA sequencing for MRD assessment, enabling sensitive, longitudinal monitoring of fusion transcripts and expression-based biomarkers within a single streamlined assay.

Further information **contact@ogt.com | ogt.com | Oxford Gene Technology Ltd., Unit 5, Oxford Technology Park, 4A Technology Drive, Kidlington, Oxfordshire, OX5 1GN, UK**

SureSeq: For Research Use Only; Not for Diagnostic Procedures. © Oxford Gene Technology IP Limited – 2026.

Learn more about the fusion MRD panel